

Asymmetric predictability in causal discovery: an information theoretic approach.

Soumik Purkayastha*

Department of Biostatistics, University of Michigan
and

Peter X. K. Song†

Department of Biostatistics, University of Michigan

October 27, 2022

Abstract

Causal investigations in observational studies pose a great challenge in scientific research where randomized trials or intervention-based studies are not feasible. Leveraging Shannon’s seminal work on information theory, we develop a causal discovery framework of “predictive asymmetry” for bivariate (X, Y) . Predictive asymmetry is a central concept in information geometric causal inference; it enables assessment of whether X is a stronger predictor of Y or *vice-versa*. We propose a new metric called the Asymmetric Mutual Information (AMI) and establish its key statistical properties. The AMI is not only able to detect complex non-linear association patterns in bivariate data, but also is able to detect and quantify predictive asymmetry. Our proposed methodology relies on scalable non-parametric density estimation using fast Fourier transformation. The resulting estimation method is manyfold faster than the classical bandwidth-based density estimation, while maintaining comparable mean integrated squared error rates. We investigate key asymptotic properties of the AMI methodology; a new data-splitting technique is developed to make statistical inference on predictive asymmetry using the AMI . We illustrate the performance of the AMI methodology through simulation studies as well as multiple real data examples.

Keywords: Copula, Data splitting inference, Direction of association, Entropy, Mutual information.

*soumikp@umich.edu

†pxsong@umich.edu

1 Introduction

The discovery of causal relationships from observational data is a cornerstone of scientific research. Given observations on bivariate (X, Y) , a fundamental question of interest is to determine whether an observed statistical dependence may be explained by a causal influence of either X on Y or *vice-versa*. This investigation requires three critical assumptions in observational studies, namely positivity, consistency and ignorability (Imbens and Rubin, 2015), that are not verifiable, and existing sensitivity analyses can only provide limited capacities of assessing the validity of these conditions. Thus, such limitations pose a great challenge in the causal analysis of observational data. Even under simplifying assumptions of no confounding, no feedback loops, and no selection bias (Pearl, 2000), directly assessing bivariate causal relationship is a notoriously hard problem (Spirtes and Zhang, 2016). Although the gold standard for detecting causality involves controlled experimentation, in many cases, such trials are prohibitively expensive, technically challenging or even unethical. In the absence of domain knowledge on causality, we hope to track, capture and evaluate certain statistical features from observational data to find potential signs of causal directions (Mooij et al., 2016). This paper focuses on one key feature: asymmetry, which may be deemed as an informative reflection of underlying causality (Janzing et al., 2012).

In standard statistical problems, classical measures of association like Pearson's r , Spearman's ρ and Kendall's τ have gained their popularity for detecting linear or monotonic patterns, but they are limited when measuring complex, non-linear associations. To address this, various methods have been proposed, such as those based on joint cumulative distribution functions and ranks (Deb and Sen, 2021; Bergsma and Dassios, 2014; Rosenblatt, 1975; Hoeffding, 1948), kernel based techniques (Zhang et al., 2017; Sen and Sen, 2014), tools based on copulas (Zeng et al., 2018; Dette et al., 2013; Lopez-Paz et al., 2013),

and information theoretic metrics (Reshef et al., 2011; Kraskov et al., 2004). A common shortcoming of these methods is their inability to reveal insights on underlying causality, since their formulation is based on an implicit assumption of symmetry, i.e., in bivariate (X, Y) , one variable Y is assumed to be equally dependent on another variable X , and *vice versa*. Thus, in attempting to move further beyond traditional association studies, a critical step involves unveiling asymmetry in bivariate relationships.

Theories about causality from other fields of research such as fundamental physics (Kutach, 2013) and philosophy (Dowe, 1992) emphasize that there is an inherent sense of asymmetry in causal relations. Asymmetry in a relationship may arise when one variable plays a leading role in the sense that its alteration leads to a change in another variable. Capturing asymmetry is not equivalent to identifying causality but the former may be treated as a signpost of underlying causality. We view asymmetry as a low-dimensional representation of causality. In this paper, we propose a causal discovery instrument to study asymmetry using well-known information theoretic coefficients (Shannon, 1948) like entropy and mutual information. Further, we leverage an intrinsic connection to copula (Czado, 2019; Ma and Sun, 2008) in order to develop large-sample theory and provide interpretability.

Our methodological development is based on the following understanding of asymmetry between two variables. First, causality implies a (non-)linear and asymmetric relation but the reverse does not hold. Second, in an asymmetric relation, information flows moves from a variable with higher information relative to the variable with lower information. Third, two variables can, in principle influence each other but asymmetry implies that one variable predominantly influences over the other. Specifically, in this paper we utilize predictability to quantify influence, leading to a new metric, called the asymmetric mutual

information (*AMI*). *AMI* enables us not only to perform a statistical test for independence but also to quantify asymmetry through a notion of “asymmetric predictability” or “predictive asymmetry” and further make inference on asymmetry, if it exists. Utilizing the power of fast Fourier transformation (O’Brien et al., 2016; Bernacchia and Pigolotti, 2011), we develop a computationally fast and robust method to estimate *AMI* non-parametrically (Zeng et al., 2018). Additionally, one of our new theoretical contributions pertains to a novel statistical inference theory based on data-splitting, leading to a hypothesis test for asymmetry. The data-splitting inference is deemed effective to handle high-dimensional nuisance parameters involved in the estimation of non-parametric density functions.

The organization of this paper is as follows. Section 2 presents the formulation of our framework. Section 3 presents the estimation methodology and theoretical guarantees. In Section 4, we present simulation studies used to evaluate the finite-sample performance of our method. We apply our method to analyze three real data examples in Section 5. Finally, we make some concluding remarks in Section 6. Detailed proofs of the large sample properties are included in the Appendix.

2 Asymmetric mutual information (AMI)

We begin with a brief review of some information theoretic quantities, namely, mutual information and entropy. With these well-known quantities, we construct the *AMI*.

2.1 Mutual information is copula entropy

Let X and Y be two random variables with joint density function f_{XY} , and f_X and f_Y be the marginal densities, respectively. The mutual information $MI(X, Y)$ (Shannon, 1948)

of these two variables takes the form:

$$MI(X, Y) = E_{XY} \left\{ \log \frac{f_{XY}(X, Y)}{f_X(X)f_Y(Y)} \right\}, \quad (1)$$

where E_{XY} denotes expectation over f_{XY} . MI is symmetric and may be used to investigate the strength of a symmetric dependence between X and Y . Some properties that make it an attractive measure of complex dependence include: (i) $MI \geq 0$ with equality if and only if X and Y are independent; (ii) a larger value of MI indicates a stronger dependence between two variables; and (iii) MI is self-equitable in the sense that it is a symmetric measure which places the same importance on linear and non-linear associations (Kinney and Atwal, 2014). We consider an equivalent formulation of MI by invoking the marginal transformations $U = F_X(X) \sim \mathcal{U}(0, 1)$ and $V = F_Y(Y) \sim \mathcal{U}(0, 1)$, where F_X and F_Y are the cumulative distribution functions (CDF) of X and Y respectively. A little algebra according to Sklar's theorem (Czado, 2019) reveals

$$MI(X, Y) = MI(U, V) = E_{\mathbf{Z}} \{ \log c(\mathbf{Z}) \}, \quad (2)$$

where $\mathbf{Z} = (U, V) \in [0, 1]^2$ and c is the unique copula density function defined on the unit square $[0, 1]^2$. Note that if we assume knowledge of the estimator \hat{c} of c , estimation of mutual information is equivalent to evaluating the sample mean of the log of the estimator \hat{c} at (transformed) data points $\left[\mathbf{Z}_j = \left\{ \hat{F}_X(X_j), \hat{F}_Y(X_j) \right\} \right]_{j=1}^n$ on the compact domain $[0, 1]^2$. Note that \hat{F}_X and \hat{F}_Y are the empirical cumulative distribution functions (ECDF) of X and Y respectively.

2.2 Marginal and conditional entropies

The marginal entropy of X is defined as $H(X) = E_X \{ -\log f_X(X) \}$, where E_X denotes expectation over f_X , while the conditional entropy of X conditioned on Y is given by

$H(X|Y) = H(X, Y) - H(Y)$, where $H(X, Y) = E_{XY} \{-\log f_{XY}(X, Y)\}$ is the joint entropy of (X, Y) . These quantities are related to $MI(X, Y)$ via the following identities:

$$\begin{aligned} MI(X, Y) &= H(X) + H(Y) - H(X, Y), \\ H(X, Y) &= MI(X, Y) + H(X|Y) + H(Y|X). \end{aligned} \tag{3}$$

$H(X)$ measures the uncertainty of a random variable X , while $H(X|Y)$ measures the uncertainty of a random variable X given knowledge of another random variable Y . It is known that $H(X|Y) > H(Y|X)$ implies conditioning on X and predicting Y yields less uncertainty (Cover and Thomas, 2005), thereby establishing a sense of “asymmetric predictability”. Under independence of X and Y , we have (i) $MI = 0$, $H(X|Y) = H(X)$ and $H(Y|X) = H(Y)$. As in Section 2.1, estimating entropy $H(X)$ is straightforward if we assume knowledge of the estimator \hat{f}_X , where we evaluate the sample mean of the log of the estimator \hat{f}_X at data points $\{X_j\}_{j=1}^n$.

2.3 Entropy ratio

The entropy decomposition in Equation (3) resembles Fisher’s seminal decomposition of the total variation into the sum of within and between variations in the analysis of variance (ANOVA) framework. The decomposition plays an important role in developing a metric to quantify asymmetric predictability in the bivariate relationship: the total entropy $H(X, Y)$ may be decomposed to establish a sense of “symmetric behaviour” through $MI(X, Y)$ and “asymmetric behaviour” through $H(X|Y)$ and $H(Y|X)$. Assuming X and Y are not independent, (i.e., $MI \neq 0$), we propose a new formulation of asymmetric predictability between X and Y : an asymmetry between X and Y emerges if $H(Y|X) \neq H(X|Y)$. Further, if the uncertainty of $X|Y$ is more (less) than the uncertainty of $Y|X$, we posit that X is more (less) predictive than Y in the bivariate relationship. As a result, it reveals

which of X or Y has a more dominant predictive role to play in driving a departure from a symmetric relationship. To formally assess this departure, we define the entropy ratio of X relative to Y , denoted by $ER(X|Y)$, as follows:

$$ER(X|Y) = \frac{\exp\{H(X|Y)\}}{[\exp\{H(X|Y)\} + \exp\{H(Y|X)\}]}, \quad (4)$$

where the exponential transformation guarantees all components of $ER(X|Y)$ are positive. It is easy to see that (i) $ER(X|Y) = ER(Y|X) = 1/2$ if and only if $H(X|Y) = H(Y|X)$ and (ii) $ER(X|Y) \leq ER(Y|X)$ implies $H(X|Y) \leq H(Y|X)$, with $H(Y|X) < H(X|Y)$ establishing X as the “dominant predictor variable” that exerts more “influence” on Y . Comparing conditional entropies is motivated by recent advances in Information-Geometric Causal Inference (IGCI), where a key idea involves comparing $H(X) \leq H(Y)$ (Janzing et al., 2012). A little algebra reveals a chain of equivalence as follows:

$$ER(X|Y) \leq ER(Y|X) \iff H(X|Y) \leq H(Y|X) \iff H(X) \leq H(Y),$$

thus providing a motivation for comparing $ER(X|Y) \leq ER(Y|X)$ (see Janzing et al. (2012); Daniusis et al. (2012) for more details). In brief, IGCI-based approaches assign a causal direction from X to Y if $H(X|Y) > H(Y|X) \iff H(X) > H(Y)$

Metrics similar to our $ER(X|Y)$ in Equation (4) are scattered in the statistical literature. One example is the work on modeling asymmetric exchange of citations between two statistical research journals (Varin et al., 2015). The authors aim to build a knowledge network by modeling how much ‘influence’ one journal J_1 exerts on another journal J_2 by means of citations using the Stigler model (Stigler, 1994). The proposed model incorporates both the total number of citations jointly exchanged between two journals (a symmetric measure) as well as an asymmetric “export score” that either journal has relative to the other.

Proposition 1. *Transitive property of ER: Let us assume for three variables (X, Y, Z) , where the three pairwise $MI(X, Y)$, $MI(Y, Z)$, $MI(X, Z)$ are all non-zero. We assume X is more predictive than Y , i.e., $ER(X|Y) > 1/2$ and Y is more predictive than Z , i.e., $ER(Y|Z) > 1/2$. This yields $ER(X|Z) > 1/2$.*

Proof. The inequality $ER(X|Y) > 1/2$ implies $H(X|Y) > H(Y|X) \iff H(X) > H(Y)$ and the inequality $ER(Y|Z) > 1/2$ establishes $H(Y) > H(Z)$. Together, this yields $H(X) > H(Z)$, which further implies $H(X|Z) > H(Z|X) \iff ER(X|Z) > 1/2$. In other words, an ordering of ER between (X, Y) and (Y, Z) provides insight on direction of dependence in a third pair, i.e., (X, Z) within our proposed framework. \square

2.4 Asymmetric mutual information

We now propose a new measure called the *asymmetric mutual information* (AMI) that fulfills two primary analytic objectives: (i) test for independence of two random variables and (ii) establish asymmetric predictability in bivariate (X, Y) . The AMI of two variables X and Y is defined by:

$$AMI(X|Y) = MI(X, Y) \times ER(X|Y). \quad (5)$$

We establish some key properties of AMI :

- $AMI(X|Y) \geq 0$ and $AMI(Y|X) \geq 0$. They are simultaneously zero if and only if X and Y are independent. This forms the basis for testing statistical independence of X and Y .
- $AMI(X|Y) \leq AMI(Y|X)$ implies $ER(X|Y) \leq ER(Y|X)$, which, under our proposed tenet of asymmetric predictability, naturally establishes whether X or Y is the “dominant predictor variable”. We consider the following quantity to test for

asymmetric predictability:

$$\Delta = AMI(X|Y) - AMI(Y|X). \quad (6)$$

Consequently, when $MI \neq 0$, comparing $\Delta \leq 0 \Leftrightarrow AMI(X|Y) \leq AMI(Y|X) \Leftrightarrow H(X|Y) \leq H(Y|X)$, establishes a natural ordering in (X, Y) . Specifically, $\Delta > 0$ implies X as the dominant predictor variable over Y , resulting in a certain direction of dependence between the two variables. $\Delta < 0$ implies the converse.

Intuitively, our new estimator $AMI(X|Y)$ is a scaled function of MI , which is an effective tool to capture symmetric association. The scaling factor $ER(X|Y)$ aims to capture asymmetric behaviour between X and Y by comparing their relative predictive performance when they are associated.

3 Methodology

In order to estimate the AMI , we first tackle the problem of estimating a continuous density from a set of bivariate data points. Kernel density estimators (KDEs) are commonly used techniques for estimating the probability density function (PDF). The KDE method requires specification of some kind of bandwidth or a kernel function with a specific bandwidth. Bandwidth selection is a tricky issue and it calls for user-intervention for common use cases (Silverman, 1986). Further, bandwidth tuning is computationally intensive, since it requires repeated density estimation. The difficulty compounds for higher dimensions (Duong and Hazelton, 2005). A review of automatic selection methods (Heidenreich et al., 2013) recommends a variety of different approaches that are dependent on data set characteristics (including sample size, distribution smoothness, and skewness) and thus is hard to implement in practise.

An attractive alternative to the kernel-based estimation strategy involves Fourier transformation. [Bernacchia and Pigolotti \(2011\)](#) presented a solution for objectively and optimally choosing both the kernel shape and bandwidth in one dimension and [O’Brien et al. \(2016\)](#) extended the method to higher dimensions. This extension provides a data-driven bivariate PDF estimation method that is fast and unencumbered by the need for user-selected parameters. The estimator so obtained, is called the self-consistent estimator (SCE), and is used to estimate our *AMI* coefficient.

3.1 The self-consistent density estimator

Let us consider a random bivariate sample denoted by $\mathcal{S} = \{\mathbf{X}_j : \mathbf{X}_j \in \mathcal{X}, j = 1, 2, \dots, n\}$ from density f , which belongs to the Hilbert space of square integrable functions (denoted by $\mathcal{L}^2 = \{f : \int f^2(\mathbf{x})d\mathbf{x} < \infty\}$). Without loss of generality, $\mathcal{X} = \mathbb{R}^2$.

We consider the SCE $\hat{f} \in \mathcal{L}^2$. In order to define \hat{f} , we require a kernel function K , which belongs to the class of functions given by

$$\mathcal{K} := \left\{ K : K(\mathbf{x}) \geq 0 \forall \mathbf{x}; K(\mathbf{x}) = K(-\mathbf{x}) \forall \mathbf{x}; \int K(\mathbf{t})d\mathbf{t} = 1 \right\}.$$

Specifically, \hat{f} is given by the convolution of a kernel K and the set of delta functions centered on the dataset as follows:

$$\begin{aligned} \hat{f}(\mathbf{x}) &:= n^{-1} \sum_{j=1}^n K(\mathbf{x} - \mathbf{X}_j), \quad \mathbf{x} \in \mathcal{X} \\ &= n^{-1} \sum_{j=1}^n \int_{\mathcal{X}} K(\mathbf{s})\delta(\mathbf{x} - \mathbf{X}_j - \mathbf{s})d\mathbf{s}, \end{aligned} \tag{7}$$

where $\delta(\mathbf{x})$ is the Dirac delta function ([Kreyszig, 2020](#)). For more discussion on $\delta(\mathbf{x})$ see Section S1.1 of the Supplement.

Our aim is identify the optimal kernel \hat{K} , where “optimal” is intended as minimising

the mean integrated square error (*MISE*) between the true density f and the estimator \hat{f} :

$$\begin{aligned} \hat{K} &:= \operatorname{argmin}_{K \in \mathcal{K}} \operatorname{MISE}(\hat{f}, f) \\ &= \operatorname{argmin}_{K \in \mathcal{K}} \mathbb{E} \left[\int_{\mathbb{R}^p} \{\hat{f}(\mathbf{x}) - f(\mathbf{x})\}^2 d\mathbf{x} \right], \end{aligned} \tag{8}$$

where the \mathbb{E} operator denotes taking expectation over the entire support of f .

The SCE in Equation (7) may be represented equivalently by its inverse Fourier transform pair, $\hat{\phi} \in \mathcal{L}^2$:

$$\hat{\phi}(\mathbf{t}) = \mathcal{F}^{-1}(\hat{f}(\mathbf{x})) = \kappa(\mathbf{t})\mathcal{C}(\mathbf{t}), \tag{9}$$

where \mathcal{F}^{-1} represents the multidimensional inverse Fourier transformation from space of data $\mathbf{x} \in \mathbb{R}^2$ to frequency space coordinates $\mathbf{t} \in \mathbb{R}^2$. $\kappa = \mathcal{F}^{-1}(K)$ is the inverse Fourier transform of the kernel K and \mathcal{C} is the empirical characteristic function (ECF) of the data, defined as

$$\mathcal{C}(\mathbf{t}) = n^{-1} \sum_{j=1}^{n_1} \exp(it' \mathbf{X}_j). \tag{10}$$

[Bernacchia and Pigolotti \(2011\)](#) derive the optimal transform kernel $\hat{\kappa}$ that minimizes the *MISE* in Equation (8), given as follows:

$$\hat{\kappa}(\mathbf{t}) = \frac{n}{2(n-1)} \left[1 + \sqrt{1 - \frac{4(n-1)}{|n\mathcal{C}(\mathbf{t})|^2}} \right] I_{A_n}(\mathbf{t}). \tag{11}$$

Note that A_n serves as a low-pass filter that yields a stable estimator (see Sections S1.2 and S1.3 of the Supplement). We follow the nomenclature of [Bernacchia and Pigolotti \(2011\)](#), and denote A_n as the set of ‘‘acceptable frequencies’’. For further discussion on A_n please see Section 1.3 of the Supplement.

The optimal transform kernel $\hat{\kappa}$ in Equation (11) may be antitransformed back to the real space to obtain the optimal kernel \hat{K} , which also belongs to \mathcal{K} . The classical kernel estimation approach (see [Silverman \(1986\)](#)) assumes a specific form (such as the Gaussian kernel or Epanechnikov kernel) of the kernel K_H which depends on a bandwidth parameter

H and requires tuning H according to some optimality criterion. In contrast, the SCE method does not make strong assumptions on the functional form of K . Rather, its estimate \hat{K} will be determined entirely by a data-driven approach.

We state the sufficient conditions for the estimate \hat{f} to converge to the true density f for $n \rightarrow \infty$. Theorem 1 establishes strong consistency of the estimator \hat{f} to the true density f as $n \rightarrow \infty$ at all points on the support of f .

Theorem 1. *Let the true density f be square integrable and its corresponding Fourier transform ϕ be integrable, then the self consistent estimator \hat{f} , which is defined by Equations (7) - (11) converges almost surely to the true density as $n \rightarrow \infty$, under the additional assumptions $\mathcal{V}(A_n) \rightarrow \infty$, $\mathcal{V}(A_n)/\sqrt{n} \rightarrow 0$ and $\mathcal{V}(\bar{A}_n) \rightarrow 0$ as $n \rightarrow \infty$. Further, assuming f to be continuous on support χ , we have uniform almost sure convergence of \hat{f} to f as $n \rightarrow \infty$.*

Proof. Here A_n represents the frequency filter that ensures a stable solution of the SCE \hat{f} . \bar{A}_n is the complement of A_n and the volume of A_n is given by $\mathcal{V}(A_n)$. The detailed proof of Theorem 1 is given in Section S1.4 of the Supplement. \square

3.2 Asymptotic normality

An examination of Equations (5) and (6) reveals that in order to estimate $AMI(X|Y)$, we need to estimate two quantities, namely $MI(X, Y)$ and $ER(X|Y)$. To establish the asymptotic normality of the resulting estimators \widehat{AMI} and $\hat{\Delta}$, we propose a data-splitting technique as described below. Note that the data-splitting technique is solely for statistical inference and not required for estimation purposes.

We split the data of size n into two disjoint sets, \mathcal{D}_1 and \mathcal{D}_2 with sample sizes n_1 and n_2 respectively ($n_1 + n_2 = n$). As described in Section 3.1, using data from \mathcal{D}_1 we obtain

estimates of the copula density function $\hat{c}_{\mathcal{D}_1}$ and the marginal density functions $\hat{f}_{X;\mathcal{D}_1}$ and $\hat{f}_{Y;\mathcal{D}_1}$. Under some mild assumptions (see Theorem 1), we have proved uniform almost sure convergence of these estimators to their population counterparts on their respective support sets as sample size $n_1 \rightarrow \infty$. Using data from \mathcal{D}_2 , we then evaluate the estimators $\widehat{MI}(X, Y)$, $\hat{H}(X)$ and $\hat{H}(Y)$ as follows

$$\begin{aligned}\widehat{MI}(X, Y) &= n_2^{-1} \sum_{j=1}^{n_2} \log \{ \hat{c}_{\mathcal{D}_1}(\mathbf{Z}_j^{D_2}) \}, \\ \hat{H}(X) &= n_2^{-1} \sum_{j=1}^{n_2} -\log \{ \hat{f}_{X;\mathcal{D}_1}(X_j^{D_2}) \}, \\ \hat{H}(Y) &= n_2^{-1} \sum_{j=1}^{n_2} -\log \{ \hat{f}_{Y;\mathcal{D}_1}(Y_j^{D_2}) \},\end{aligned}\tag{12}$$

where the original data points are given by $\{(X_j, Y_j)\}_{j=1}^n$ and transformed (to copula space $[0, 1]^2$) data points are given by $\{\mathbf{Z}_j\}_{j=1}^n$. Consequently, the estimators of AMI and Δ are given as follows

$$\begin{aligned}\widehat{AMI}(X|Y) &= \widehat{MI}(X, Y) \times \widehat{ER}(X|Y), \\ \widehat{AMI}(Y|X) &= \widehat{MI}(X, Y) \times \widehat{ER}(Y|X), \\ \hat{\Delta} &= \widehat{AMI}(X|Y) - \widehat{AMI}(Y|X).\end{aligned}\tag{13}$$

The following theorem establishes asymptotic normality of $\widehat{AMI}(X|Y)$ as $n_1 \wedge n_2 := \min(n_1, n_2) \rightarrow \infty$.

Theorem 2. *Let the conditions presented in Theorem (1) hold. We assume that the true copula density c and marginal densities f_X and f_Y are smooth and bounded away from zero and infinity on their respective support. Further, we assume $MI \neq 0$. Under these assumptions, we have*

$$\sqrt{n_2} \left\{ \widehat{AMI}(X|Y) - AMI(X|Y) \right\} \xrightarrow{\mathcal{D}} N(0, \sigma_{AMI}^2),$$

as $n_1 \wedge n_2 \rightarrow \infty$, with σ_{AMI}^2 denoting the asymptotic variance of the estimator.

Proof. The proof of Theorem 3 is given in Section S2.2 of the Supplement, which also presents a closed-form expression of σ_{AMI}^2 . \square

A similar result holds for $\hat{\Delta}$, as is described by the following theorem.

Theorem 3. *Let the conditions presented in Theorem (3) hold. Under these assumptions, we have*

$$\sqrt{n_2} \left(\hat{\Delta} - \Delta \right) \xrightarrow{\mathcal{D}} N(0, \sigma_{\Delta}^2),$$

as $n_1 \wedge n_2 \rightarrow \infty$, with σ_{Δ}^2 denoting the asymptotic variance of the estimator.

Proof. The proof of Theorem 3 is included in Section S2.5 of the Supplement, which also presents a closed-form expression of σ_{Δ}^2 . \square

Remark 1. *Note that the sample size-based scaling factor associated with both $\hat{\Delta}$ and \widehat{AMI} are linked with the sample size n_2 of the second data split \mathcal{D}_2 , rather than the entire combined sample $n = n_1 + n_2$. This is a consequence of the data splitting method we propose. However, we require $n_1 \wedge n_2 \rightarrow \infty$ while analysing the asymptotic behaviour of $\hat{\Delta}$ and \widehat{AMI} . For all results presented in this paper, we split the data to create two datasets of (approximately) similar size, i.e., $(n_1 = n_2) \approx n/2$.*

3.3 Testing for independence using AMI

The proposed statistic $\widehat{AMI}(X|Y) = \widehat{MI}(X, Y) \times \widehat{ER}(X|Y)$ is used to test for independence between two variables X and Y . Rejection rules of the test based on asymptotic theory require data with large sample sizes, which may not be always available in practice. To ensure a stable and reliable performance, we implement a permutation-based test as it can give a precise finite-sample distribution of the test statistic for even small samples (Manly, 2018). For a random sample of n observations, $S = \{(X_j, Y_j)\}_{j=1}^n$, let

$\{\delta(1), \delta(2), \dots, \delta(n)\}$ be a random permutation of $\{1, 2, \dots, n\}$. Based on δ -permuted data set $S_\delta = \{(X_j, Y_{\delta(j)})\}_{j=1}^n$, we calculate the corresponding estimate \widehat{AMI}_{δ_1} . On repeating the above procedure r times, $\mathcal{T}_{perm} = \{\widehat{AMI}_{\delta_r}\}_{r=1}^R$, a collection of the AMI estimates is obtained. The null distribution of \widehat{AMI} , under the null hypothesis $H_0 : X$ and Y are independent, can be approximated by the empirical distribution generated by \mathcal{T}_{perm} . At significance level α , we reject the null hypothesis when \widehat{AMI} based on the original data is greater than the $(1 - \alpha)$ th empirical quantile of \mathcal{T}_{perm} . With the null hypothesis rejected, we may further test for the asymmetric predictability as described in the next section.

3.4 Test for asymmetric predictability using Δ

The difference $\Delta(X|Y) = AMI(X|Y) - AMI(Y|X)$ determines a direction of dependence between X and Y . When X and Y are not independent, with both $AMI(X|Y) > 0$ and $AMI(Y|X) > 0$, the null hypothesis $H_0 : \Delta = 0$ signifies a bivariate relationship with “predictive symmetry”. If Δ is significantly larger (smaller) than zero, then we assign a direction of dependence from Y to X (X to Y) since X (Y) exerts “predictive dominance” on Y (X). We propose an asymptotic test based on the large sample behaviour of $\hat{\Delta}$ to test for the null hypothesis H_0 described above. Using the result presented in Theorem (3), we may obtain a $100(1 - \alpha)\%$ asymptotic confidence interval (CI) of Δ . If the CI contains zero, we claim X and Y have predictive symmetry. If the CI lies to the right (left) of zero, we acquire data evidence in favor of $AMI(X|Y)$ being significantly larger (smaller) than $AMI(Y|X)$. Consequently, we assert, at α level of significance, that X exerts predictive dominance over Y (Y exerts predictive dominance over X) in their bivariate asymmetric relationship.

4 Simulation studies

4.1 Testing for independence

We use synthetic datasets to evaluate the performance of the *AMI*-based test for independence in a bivariate framework. In the following, let $S = \{(X_j, Y_j)\}_{j=1}^n$ be a random sample of n observations drawn from a bivariate PDF f_{XY} on \mathbb{R}^2 . For each of the bivariate associations described below, we simulate the data via the decomposition $f_{X,Y} = f_{Y|X} \times f_X$ where $f_{Y|X}$ is the conditional PDF of Y conditioned on X and f_X is the marginal PDF of X . Similar to [Zeng et al. \(2018\)](#), in each pattern described below, the signal parameter a determines strength of association between X and Y with $a = 0$ denoting independence. Upon increasing a , we increase the signal strength of X in Y relative to the independent noise ϵ , i.e., we increase the signal-to-noise ratio, implying a departure from independence (i.e. the null case). In Supplementary Figure F1, we present scatter plots of each of the eight patterns considered, over various values of a , exhibiting various association patterns from linear to highly nonlinear relationships.

P1. Linear with symmetric noise: $X \sim N(0, 1)$ and $Y = aX + \epsilon$, $\epsilon \sim N(0, 0.5)$.

P2. Linear with asymmetric noise: $X \sim N(0, 1)$ and $Y = aX + (\epsilon - 1)$, $\epsilon \sim \text{Exp}(1)$.

P3. Quadratic with symmetric noise: $X \sim N(0, 1)$ and $Y = aX^2 + \epsilon$, $\epsilon \sim N(0, 0.5)$.

P4. Quadratic with asymmetric noise: $X \sim N(0, 1)$ and $Y = aX^2 + (\epsilon - 1)$, $\epsilon \sim \text{Exp}(1)$.

P5. Circular with symmetric noise: $\theta \sim U(0, 1)$, $X = 3 \cos(2\pi\theta)$ and $Y = 3a \sin(2\pi\theta) + \epsilon$,
 $\epsilon \sim N(0, 1)$.

P6. Spiral with symmetric noise: $\theta \sim U(0, 4)$, $X = a\theta \cos(\pi\theta) + \epsilon_1$ and $Y = \theta \sin(\pi\theta) + \epsilon_2$,
 $\epsilon_1 \sim N(0, 0.1)$, $\epsilon_2 \sim N(0, 0.1)$.

P7. Exponential with symmetric noise: $U \sim U(-3, 3)$, $X = U + \epsilon_1$ and $Y = a \exp(U) + \epsilon_2$,
 $\epsilon_1 \sim N(0, 0.1)$, $\epsilon_2 \sim N(0, 0.1)$.

P8. Sinusoidal with symmetric noise: $U \sim U(0, \sqrt{12})$, $X = U + \epsilon_1$ and $Y = a \sin(2\pi U / \sqrt{12}) + \epsilon_2$, $\epsilon_1 \sim N(0, 0.1)$, $\epsilon_2 \sim N(0, 0.1)$.

In each pattern above, the systematic components are independent of the error components. For each scenario described above, we examine the performance of the *AMI*-based permutation test for independence through both type I error rate under the null case, i.e., independence, with $a = 0$ and the empirical power curve for different values of a summarized from $r = 1000$ rounds of simulation. We vary sample sizes $n \in \{250, 500, 1000\}$.

The results are presented in Figure 4.1. Note that the test returns a size that is approximately at the nominal $\alpha = 0.05$ under the null hypothesis of independence, exhibiting control over Type I error. In each scenario described above, increasing the strength of association in (X, Y) results in increased empirical power of the test. Simulating data from the linear association pattern P1 and P2, given the same value of a , the test detects independence for asymmetric noise with higher power than for symmetric noise. A similar observation is made for quadratic association patterns P3 and P4 as well. Moreover, with no surprise, the empirical power increases as we increase sample size in all the examples considered.

4.2 Testing for predictive asymmetry

We examine the test for predictive asymmetry introduced in Section 3.4, which is the main focus of this paper. Using the statistic $\hat{\Delta}(X|Y) = \widehat{AMI}(X|Y) - \widehat{AMI}(Y|X)$, we want to investigate departure from symmetric association in synthetic bivariate datasets. We generate a sample of n observations drawn from a bivariate PDF f_{XY} on \mathbb{R}^2 , through

representation involving Sklar’s theorem the underlying copula density function and the two associated marginal densities, given as follows:

1. Choice of copula density function: we restrict ourselves to three copula density functions - the bivariate Gaussian copula density function with parameter $\rho = 0.5$, the Clayton copula with parameter $\theta = 2$ and the Gumbel copula with parameter $\theta = 2$. For more details on various copula classes, please see [Czado \(2019\)](#); [Joe \(2014\)](#).

2. Choice of marginals: while the copula density function induces a symmetric association between X and Y , choice of the marginal densities (which influences marginal and conditional entropy) controls departure from “symmetric” association in the proposed information theoretic framework. We consider three different types of marginal density functions - the symmetric Gaussian density function $N(0, \sigma)$, the positively skewed $\text{Exp}(\text{rate} = \lambda)$, and the negatively skewed $\text{Log-Exponential}(\text{scale} = \gamma)$. Note that if $X \sim \text{Exp}(\text{scale} = \gamma)$, then $Y = \log(X)$ follows a log-exponential distribution with scale parameter γ .

We vary the parameters σ , λ and γ over a range of values. Note that by increasing the rate parameter λ for the exponential distribution as well as the scale parameter γ for the log exponential distribution yield decreased marginal (and conditional) entropy values. In contrast, increasing σ results in increased entropy values in the Gaussian marginal choice. For a given association pattern (with specified copula density parameter as well as marginal density parameters), we generate $R = 1000$ bivariate *i.i.d.* samples on (X, Y) , each of size $n = 500$, in order to draw summary statistics. For each simulated sample, we study the estimate $\left\{ \hat{\Delta}_r(X|Y) \right\}_{r=1}^R$ and compute the mean and quantile-based 95% confidence interval of $\hat{\Delta}_r$. Further, in accordance with [Theorem 3](#), we compute the theoretical versions of the 95% confidence interval as well and note that the simulation-based estimates and theoretical

values align closely with one another in all simulation cases considered. In Figure 4.2, we consider scatter plots of some specific choices of the copula and marginal distributions. Further, we report the behaviour of $\hat{\Delta}$, simulation-based 95% confidence intervals as well as computed theoretical 95% asymptotic confidence intervals. Supplementary Figures F2, F3 and F4 present a more detailed set of simulation results for all joint copula and marginal density choices.

We note in our experiments that the $\hat{\Delta}$ statistic behaves similarly regardless of the underlying copula family chosen, thereby establishing an effective tool to investigate departure from association with “predictive symmetric” in bivariate datasets: our simulation results depend only on how we specify the marginal (and hence, conditional) density functions.

We note that $\hat{\Delta}$ captures departure from association with “predictive symmetry” in bivariate datasets: our simulation results vary based on how we specify the marginal (and hence, conditional) density functions and not on the underlying copula family. Subplots (A1), (A2), (A3), and (A4), display density heatmaps of some of the bivariate distributions considered. Subplots (B1), (B2), (B3), and (B4) examine behaviour of $\hat{\Delta}$ upon changing the marginal parameters which influence asymmetric predictability in our framework. In (B1) and (B3), both marginals are either exponential or log-exponential. Note that increasing (or decreasing) the X -marginal parameter while keeping the Y -marginal fixed causes the conditional entropy of X relative to Y to decrease (or increase), since increasing λ for exponential and γ for log-exponential distributions causes the associated entropy to decrease. In (B2), for $\lambda = 0.75$ and $\sigma = 0.88$, we report a symmetric bivariate association. Upon increasing (or decreasing) σ we note an increase (or decrease) in the marginal entropy of X and hence a positive (or negative) $\hat{\Delta}$, implying predictive dominance of X over Y (Y over X), since increasing σ for normal distributions causes the associated entropy

to increase. Similarly, in (B4), for $\gamma = 0.88$ and $\sigma = 1.25$, we report a balanced bivariate association. Upon increasing (or decreasing) σ we note an increase (or decrease) in the conditional entropy of X relative to Y and hence a positive (or negative) $\hat{\Delta}$ implying predictive dominance of X over Y (or Y over X).

5 Real data application

In this section we analyse two real data sets to illustrate the usefulness of the *AMI* methodology. An third data analysis is included in the Supplement. The first example is based on the Abalone data set (Nash et al., 1994) and is taken from a benchmarked CauseEffectPairs (CEP) repository (Mooij et al., 2016). The CEP repository consists of different “cause-effect pairs”, each one consisting of samples of a pair of statistically dependent random variables, where one variable is known to cause the other one. The repository provides identifying information on “cause” and “effect” variables. The second example is based on the Early Life Exposures in Mexico to Environmental Toxicants (ELEMENT) cohort study (Perng et al., 2019). A question of interest is the direction of dependence between DNA methylation (DNAm) alterations and cardiometabolic outcomes. Specifically, our analysis focuses on a target gene *ATP2B1* that is known to be linked with blood pressure (BP) (dan Ji et al., 2021). We investigate whether DNAm alterations of this target gene lead to changes in BP or if the converse is true (Dicorpo et al., 2018). Focusing on CpG sites of this BP-related gene, we apply the *AMI* approach and hope to unveil a predictive asymmetry between CpG sites and BP variation.

5.1 The Abalone dataset

This data set contains $n = 4177$ measurements of several morphometric variables concerning the sea snail Abalone. The original data set contains variables relating to sex, length, diameter, height, weight and number of rings. Except for the categorical variable sex, all the other variables are continuous. The number of rings in the shell is directly related to the age of the snail: adding 1.5 to the number of rings a snail yields its age in years. Of these variables, we selected four pairs with established cause-effect relationships for a confirmatory analysis: age-length, age-diameter, age-height and age-weight. In this setting, we note that for the variable “age”, there is no possibility of implementing an intervention, since we cannot vary time. We expect common agreement on the ground truth: varying age results in changes to all the other variables related to length, diameter height and weight.

Figure 5.1 indicates that our *AMI* method is able to establish that age has a causal influence on all the other variables under study, judging the estimated $\hat{\Delta}$ (and 95% CI) for the four pairs. All values in Figure 5.1 are reported below, and have been multiplied by 100 in order to improve readability. We find that age predominates the pairwise relationship in all four pairs: (i) for the age-length pair, $\hat{\Delta}$ (and 95% CI) = 34.67 (21.08, 48.26); (ii) for the age-diameter pair, $\hat{\Delta} = 73.94$ (46.36, 101.52); (iii) for the age-height pair, $\hat{\Delta} = 38.42$ (24.6, 52.24); and (iv) for the age-weight pair, $\hat{\Delta} = 27.67$ (19.43, 36.01). Our results are in a full agreement with their existing cause-effect relationships in the CEP repository.

5.2 The ELEMENT dataset: asymmetry of DNAm and BP

This second analysis considers a cohort of 525 children of age 10 - 18 years in the ELEMENT cohort. We select a target gene, namely *ATP2B1*, that has been reported to be significantly associated with both systolic BP (SBP) and diastolic BP (DBP) by at least 20 independent

studies (e.g., [Plotnikov et al. \(2022\)](#); [Hoffmann et al. \(2016\)](#)). In our data, *ATP2B1* has 21 CpG sites that are mildly correlated, with inter-site Pearson’s correlation ranging from -0.43 to 0.57 . Using our *AMI*-based test, we obtain p -values from testing whether a given CpG site is significantly associated with SBP or DBP. All p -values obtained from the same gene are aggregated at the gene level using the Cauchy combination test ([Liu and Xie, 2019](#)) to account for inter-site correlations. Our findings reveal that the overall DNAm of *ATP2B1* is associated with DBP (p -value 0.042) at the 5% level of significance, confirming discoveries reported in the GWAS catalog ([Hindorff et al., 2009](#)).

Zooming in on associations at individual CpG sites within *ATP2B1*, we apply Bonferroni correction to account for multiple testing and find that CpG site *CG17564205* is significantly associated with DBP. Next, for this identified CpG site, we employ $\Delta = AMI(\text{DNAm}|\text{BP}) - AMI(\text{BP}|\text{DNAm})$ to examine the direction of association so to determine whether *CG17564205* influences BP, or conversely. We find that DBP exhibits predictive dominance over *CG17564205*, with $\hat{\Delta}$ (and 95% CI) = -2.14 ($-3.85, -0.42$). With most studies on DNAm and blood pressure association ([Han et al., 2016](#)) still in their infancy, the above findings present new evidence that both gene-level or CpG site-level DNAm alteration could be altered due to changes in blood pressure. This poses a new exciting scientific hypothesis for further validation investigation.

6 Concluding remarks

This paper has focused on developing a new statistical methodology to detect asymmetry in nonlinear relations - an implication that is often ignored in statistical methodology. Inferring asymmetry in bivariate data contributes an important piece of knowledge in the study of causality, but there is an unfortunate lacuna of well-justified statistical tools to quantify

this attribute. While asymmetry and causality are not equivalent, we posit that unveiling asymmetry (if present) in bivariate (X, Y) provides a low-dimensional representation of complex causality. In this paper we present a new causal discovery framework of asymmetric predictability between two random variables X and Y using *AMI*. By no means is asymmetric predictability the sole correct formalization that distinguishes between cause and effect, nor do we believe that a unique formalization exists.

The *AMI* has a simple formula and is easy to understand conceptually. The *AMI* leverages Shannon’s seminal information theory and has a simple expression involving mutual information and conditional entropies. The *AMI* may simultaneously be used to test for association as well as detect and quantify predictive asymmetry, thereby serving as an attractive causal discovery tool.

A Fast Fourier Transformation-based method (O’Brien et al., 2016; Bernacchia and Pigolotti, 2011) is used to estimate the *AMI* instead of conventional kernel-based methods. Our estimation method is completely data driven and does not incur prefixed tuning parameters, like bandwidth, despite *AMI* being a function of PDFs. Moreover, our method consistently performs faster than existing bandwidth-dependent methods - being approximately 4 orders of magnitude faster for bivariate sample sizes of approximately 10^4 . We also propose a new data-splitting method which provides theoretical justifications for key large-sample properties of *AMI*. Not only does the data-splitting technique help establish asymptotic normality for functions of PDFs, the technique is deemed effective to handle high-dimensional nuisance parameters involved in the nonparametric estimation of functions of PDFs.

The *AMI* enjoys high power for testing independence while controlling for Type I error, which is exhibited through a wide range of simulation results. The *AMI* further provides

information on asymmetry – which enhances our understanding of large and small data sets. Our simulations and data analysis clearly demonstrate the necessity and universal applicability of the quantification of asymmetric predictability in bivariate associations, thereby capturing some degree of underlying causality.

The *AMI* is currently applicable only for continuous bivariate data on (X, Y) and may be extended to discrete data with little effort. In order to account for confounding features (say, Z), we can generalize the *AMI* methodology by using the respective residuals of X and Y when they are individually regressed on Z in the calculation of *AMI*. In order to make valid inference on asymmetry, we must use data splitting, which calls for larger data sets. Our experiences from simulation studies suggested that sample sizes less than $n = 200$ are not conducive for our causal discovery framework.

We plan to distribute a well-tuned a Python package for dissemination of our toolkit. Potential applications of our *AMI* framework include mediation analysis and instrumental variable methods, in which implicit assumptions are made about causal directions, often without justification. In absence of *a priori* knowledge, our framework may serve either as a discovery or confirmatory tool, thereby aiding many applications in current scientific research, particularly in the investigation of causality.

References

- Wicher Bergsma and Angelos Dassios. A consistent test of independence based on a sign covariance related to kendall’s tau. *Bernoulli*, 20(2), May 2014. doi: 10.3150/13-bej514. URL <https://doi.org/10.3150/13-bej514>.
- Alberto Bernacchia and Simone Pigolotti. Self-consistent method for density estimation. *Journal of the Royal Statistical Society: Series B (Statistical Methodology)*, 73(3):407–

422, April 2011. doi: 10.1111/j.1467-9868.2011.00772.x. URL <https://doi.org/10.1111/j.1467-9868.2011.00772.x>.

Thomas M. Cover and Joy A. Thomas. *Elements of Information Theory*. Wiley, apr 2005. doi: 10.1002/047174882x. URL <https://doi.org/10.1002/047174882x>.

Claudia Czado. *Analyzing Dependent Data with Vine Copulas: A Practical Guide With R (Lecture Notes in Statistics, 222)*. Springer, paperback edition, 5 2019. ISBN 978-3030137847. URL <https://lead.to/amazon/com/?op=bt&la=en&cu=usd&key=3030137848>.

Lin dan Ji, Zhi feng Xu, Nelson L. S. Tang, and Jin Xu. Natural selection of ATP2b1 underlies susceptibility to essential hypertension. *Frontiers in Genetics*, 12, mar 2021. doi: 10.3389/fgene.2021.628516. URL <https://doi.org/10.3389/fgene.2021.628516>.

Povilas Daniusis, Dominik Janzing, Joris M. Mooij, Jakob Zscheischler, Bastian Steudel, Kun Zhang, and Bernhard Schölkopf. Inferring deterministic causal relations. *CoRR*, abs/1203.3475, 2012. URL <http://arxiv.org/abs/1203.3475>.

Nabarun Deb and Bodhisattva Sen. Multivariate rank-based distribution-free nonparametric testing using measure transportation. *Journal of the American Statistical Association*, 0(0):1–16, 2021. doi: 10.1080/01621459.2021.1923508. URL <https://doi.org/10.1080/01621459.2021.1923508>.

H. Dette, K. Siburg, and Pavel A. Stoimenov. A copula-based non-parametric measure of regression dependence. *Scandinavian Journal of Statistics*, 40:21–41, 2013.

Daniel A. Dicorpo, Samantha Lent, Weihua Guan, Marie-France Hivert, and James S. Pankow. Mendelian randomization suggests causal influence of glycemic traits on DNA

- methylation. *Diabetes*, 67(Supplement_1), jul 2018. doi: 10.2337/db18-1707-p. URL <https://doi.org/10.2337%2Fdb18-1707-p>.
- Phil Dowe. Process causality and asymmetry. *Erkenntnis*, 37(2), sep 1992. doi: 10.1007/bf00209321. URL <https://doi.org/10.1007%2Fbf00209321>.
- Tarn Duong and Martin L. Hazelton. Cross-validation bandwidth matrices for multivariate kernel density estimation. *Scandinavian Journal of Statistics*, 32(3):485–506, September 2005. doi: 10.1111/j.1467-9469.2005.00445.x. URL <https://doi.org/10.1111/j.1467-9469.2005.00445.x>.
- Liyuan Han, Yanfen Liu, Shiwei Duan, Benjamin Perry, Wen Li, and Yonghan He. DNA methylation and hypertension: emerging evidence and challenges. *Briefings in Functional Genomics*, page elw014, may 2016. doi: 10.1093/bfgp/elw014. URL <https://doi.org/10.1093%2Fbfgp%2Felw014>.
- Nils-Bastian Heidenreich, Anja Schindler, and Stefan Sperlich. Bandwidth selection for kernel density estimation: a review of fully automatic selectors. *AStA Advances in Statistical Analysis*, 97(4):403–433, June 2013. doi: 10.1007/s10182-013-0216-y. URL <https://doi.org/10.1007/s10182-013-0216-y>.
- Lucia A. Hindorff, Praveen Sethupathy, Heather A. Junkins, Erin M. Ramos, Jayashri P. Mehta, Francis S. Collins, and Teri A. Manolio. Potential etiologic and functional implications of genome-wide association loci for human diseases and traits. *Proceedings of the National Academy of Sciences*, 106(23):9362–9367, jun 2009. doi: 10.1073/pnas.0903103106. URL <https://doi.org/10.1073%2Fpnas.0903103106>.
- Wassily Hoeffding. A non-parametric test of independence. *The Annals of Mathematical*

Statistics, 19(4):546–557, December 1948. doi: 10.1214/aoms/1177730150. URL <https://doi.org/10.1214/aoms/1177730150>.

Thomas J Hoffmann, Georg B Ehret, Priyanka Nandakumar, Dilrini Ranatunga, Catherine Schaefer, Pui-Yan Kwok, Carlos Iribarren, Aravinda Chakravarti, and Neil Risch. Genome-wide association analyses using electronic health records identify new loci influencing blood pressure variation. *Nature Genetics*, 49(1):54–64, nov 2016. doi: 10.1038/ng.3715. URL <https://doi.org/10.1038%2Fng.3715>.

Guido W. Imbens and Donald B. Rubin. *Causal Inference for Statistics, Social, and Biomedical Sciences: An Introduction*. Cambridge University Press, hardcover edition, 4 2015. ISBN 978-0521885881. URL <https://lead.to/amazon/com/?op=bt&la=en&cu=usd&key=0521885884>.

Dominik Janzing, Joris Mooij, Kun Zhang, Jan Lemeire, Jakob Zscheischler, Povilas Daniušis, Bastian Steudel, and Bernhard Schölkopf. Information-geometric approach to inferring causal directions. *Artificial Intelligence*, 182-183:1–31, may 2012. doi: 10.1016/j.artint.2012.01.002. URL <https://doi.org/10.1016%2Fj.artint.2012.01.002>.

Harry Joe. *Dependence Modeling with Copulas (Chapman & Hall/CRC Monographs on Statistics and Applied Probability)*. Chapman and Hall/CRC, hardcover edition, 6 2014. ISBN 978-1466583221. URL <https://lead.to/amazon/com/?op=bt&la=en&cu=usd&key=1466583223>.

Justin B. Kinney and Gurinder S. Atwal. Equitability, mutual information, and the maximal information coefficient. *Proceedings of the National Academy of Sciences*, 111(9): 3354–3359, February 2014. doi: 10.1073/pnas.1309933111. URL <https://doi.org/10.1073/pnas.1309933111>.

Alexander Kraskov, Harald Stögbauer, and Peter Grassberger. Estimating mutual information. *Physical Review E*, 69(6), June 2004. doi: 10.1103/physreve.69.066138. URL <https://doi.org/10.1103/physreve.69.066138>.

Erwin Kreyszig. *Advanced Engineering Mathematics*. Wiley, loose leaf edition, 7 2020. ISBN 978-1119455929. URL <https://lead.to/amazon/com/?op=bt&la=en&cu=usd&key=1119455928>.

Douglas Kutach. Causal Asymmetry. In *Causation and its Basis in Fundamental Physics*. Oxford University Press, 09 2013. ISBN 9780199936205. doi: 10.1093/acprof:oso/9780199936205.003.0007. URL <https://doi.org/10.1093/acprof:oso/9780199936205.003.0007>.

Yaowu Liu and Jun Xie. Cauchy combination test: A powerful test with analytic p-value calculation under arbitrary dependency structures. *Journal of the American Statistical Association*, 115(529):393–402, apr 2019. doi: 10.1080/01621459.2018.1554485. URL <https://doi.org/10.1080%2F01621459.2018.1554485>.

David Lopez-Paz, Philipp Hennig, and Bernhard Schölkopf. The randomized dependence coefficient. In C. J. C. Burges, L. Bottou, M. Welling, Z. Ghahramani, and K. Q. Weinberger, editors, *Advances in Neural Information Processing Systems*, volume 26. Curran Associates, Inc., 2013. URL <https://proceedings.neurips.cc/paper/2013/file/aab3238922bcc25a6f606eb525ffdc56-Paper.pdf>.

Jian Ma and Zengqi Sun. Mutual information is copula entropy. *Tsinghua Science and Technology*, 16(1):51–54, February 2008. doi: 10.1016/s1007-0214(11)70008-6. URL [https://doi.org/10.1016/s1007-0214\(11\)70008-6](https://doi.org/10.1016/s1007-0214(11)70008-6).

- Bryan F.J. Manly. *Randomization, Bootstrap and Monte Carlo Methods in Biology*. Chapman and Hall/CRC, October 2018. doi: 10.1201/9781315273075. URL <https://doi.org/10.1201/9781315273075>.
- Joris M. Mooij, Jonas Peters, Dominik Janzing, Jakob Zscheischler, and Bernhard Schölkopf. Distinguishing cause from effect using observational data: Methods and benchmarks. *Journal of Machine Learning Research*, 17(32):1–102, 2016. URL <http://jmlr.org/papers/v17/14-518.html>.
- Warwick Nash, T.L. Sellers, S.R. Talbot, A.J. Cawthorn, and W.B. Ford. The population biology of abalone (haliotis species) in tasmania. i. blacklip abalone (h. rubra) from the north coast and islands of bass strait. *Sea Fisheries Division, Technical Report No*, 48, 01 1994.
- Travis A. O’Brien, Karthik Kashinath, Nicholas R. Cavanaugh, William D. Collins, and John P. O’Brien. A fast and objective multidimensional kernel density estimation method: fastKDE. *Computational Statistics & Data Analysis*, 101:148–160, September 2016. doi: 10.1016/j.csda.2016.02.014. URL <https://doi.org/10.1016/j.csda.2016.02.014>.
- Judea Pearl. *Causality: Models, Reasoning, and Inference*. Cambridge University Press, hardcover edition, 3 2000. ISBN 978-0521773621. URL <https://lead.to/amazon.com/?op=bt&la=en&cu=usd&key=0521773628>.
- Wei Perng, Marcela Tamayo-Ortiz, Lu Tang, Brisa N Sánchez, Alejandra Cantoral, John D Meeker, Dana C Dolinoy, Elizabeth F Roberts, Esperanza Angeles Martinez-Mier, Hector Lamadrid-Figueroa, Peter X K Song, Adrienne S Ettinger, Robert Wright, Manish Arora, Lourdes Schnaas, Deborah J Watkins, Jaclyn M Goodrich, Robin C Gar-

- cia, Maritsa Solano-Gonzalez, Luis F Bautista-Arredondo, Adriana Mercado-Garcia, Howard Hu, Mauricio Hernandez-Avila, Martha Maria Tellez-Rojo, and Karen E Peterson. Early life exposure in Mexico to Environmental toxicants (ELEMENT) project. *BMJ Open*, 9(8):e030427, Aug 2019. doi: 10.1136/bmjopen-2019-030427. URL <https://doi.org/10.1136/bmjopen-2019-030427>.
- Denis Plotnikov, Yu Huang, Anthony P. Khawaja, Paul J. Foster, Zhuoting Zhu, Jeremy A. Guggenheim, and Mingguang He. High blood pressure and intraocular pressure: A mendelian randomization study. *Investigative Ophthalmology & Visual Science*, 63(6):29, Jun 2022. doi: 10.1167/iovs.63.6.29. URL <https://doi.org/10.1167/iovs.63.6.29>.
- D. N. Reshef, Y. A. Reshef, H. K. Finucane, S. R. Grossman, G. McVean, P. J. Turnbaugh, E. S. Lander, M. Mitzenmacher, and P. C. Sabeti. Detecting novel associations in large data sets. *Science*, 334(6062):1518–1524, December 2011. doi: 10.1126/science.1205438. URL <https://doi.org/10.1126/science.1205438>.
- M. Rosenblatt. A quadratic measure of deviation of two-dimensional density estimates and a test of independence. *The Annals of Statistics*, 3(1), January 1975. doi: 10.1214/aos/1176342996. URL <https://doi.org/10.1214/aos/1176342996>.
- A. Sen and B. Sen. Testing independence and goodness-of-fit in linear models. *Biometrika*, 101(4):927–942, August 2014. doi: 10.1093/biomet/asu026. URL <https://doi.org/10.1093/biomet/asu026>.
- C. E. Shannon. A mathematical theory of communication. *Bell System Technical Journal*, 27(3):379–423, July 1948. doi: 10.1002/j.1538-7305.1948.tb01338.x. URL <https://doi.org/10.1002/j.1538-7305.1948.tb01338.x>.

B. W. Silverman. *Density Estimation for Statistics and Data Analysis*. Chapman I& Hall, London, 1986.

Peter L. Spirtes and Kun Zhang. Causal discovery and inference: concepts and recent methodological advances. *Applied Informatics*, 3, 2016.

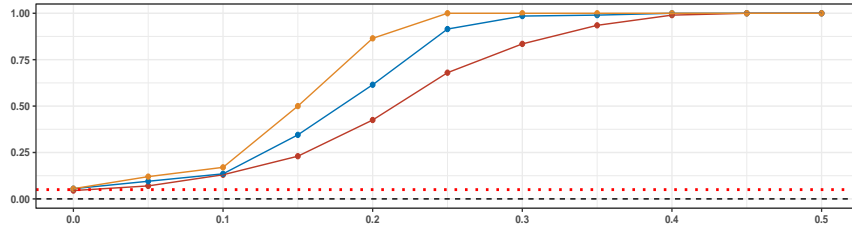
Stephen M. Stigler. Citation patterns in the journals of statistics and probability. *Statistical Science*, 9(1), February 1994. doi: 10.1214/ss/1177010655. URL <https://doi.org/10.1214/ss/1177010655>.

Cristiano Varin, Manuela Cattelan, and David Firth. Statistical modelling of citation exchange between statistics journals. *Journal of the Royal Statistical Society: Series A (Statistics in Society)*, 179(1):1–63, November 2015. doi: 10.1111/rssa.12124. URL <https://doi.org/10.1111/rssa.12124>.

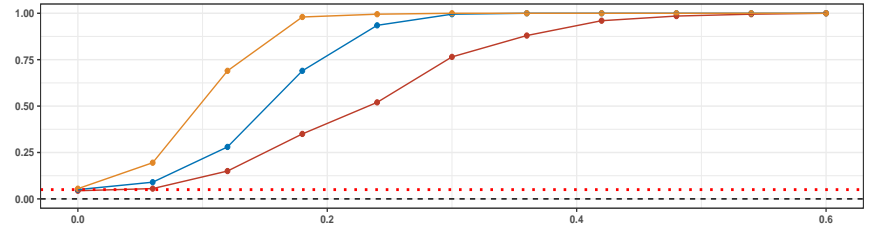
Xianli Zeng, Yingcun Xia, and Howell Tong. Jackknife approach to the estimation of mutual information. *Proceedings of the National Academy of Sciences*, 115(40):9956–9961, September 2018. doi: 10.1073/pnas.1715593115. URL <https://doi.org/10.1073/pnas.1715593115>.

Qinyi Zhang, Sarah Filippi, Arthur Gretton, and Dino Sejdinovic. Large-scale kernel methods for independence testing. *Statistics and Computing*, 28(1):113–130, January 2017. doi: 10.1007/s11222-016-9721-7. URL <https://doi.org/10.1007/s11222-016-9721-7>.

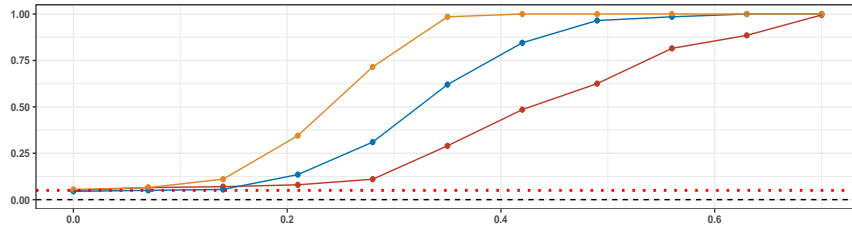
Pattern 1: linear association with symmetric noise.



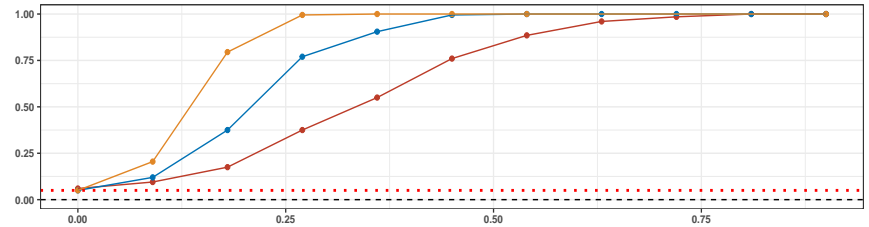
Pattern 2: linear association with asymmetric noise.



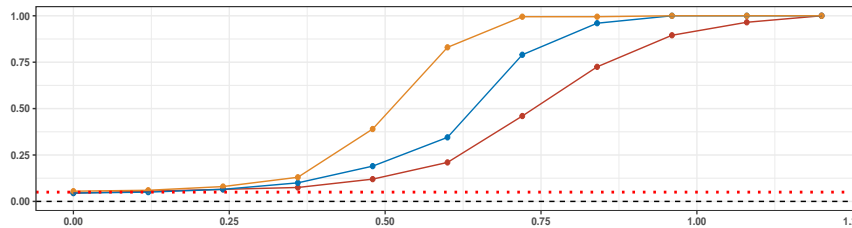
Pattern 3: quadratic association with symmetric noise.



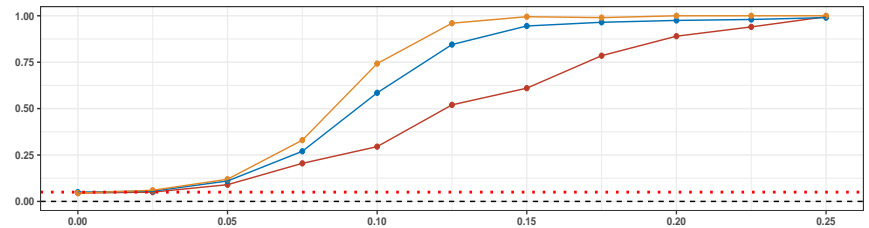
Pattern 4: quadratic association with asymmetric noise.



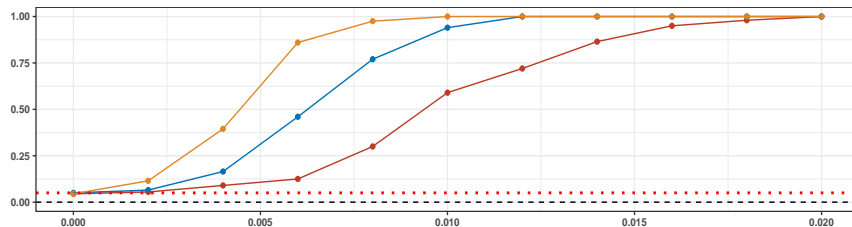
Pattern 5: circular association with symmetric noise.



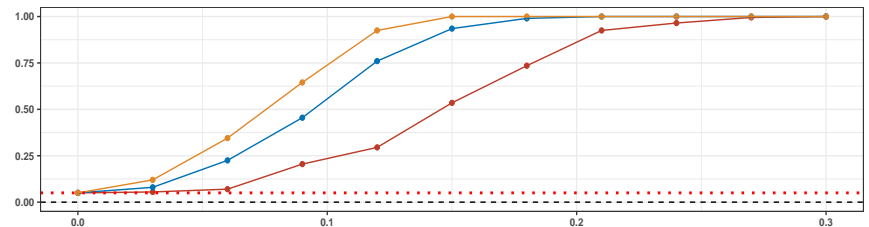
Pattern 6: spiral association with symmetric noise.



Pattern 7: exponential association with symmetric noise.



Pattern 8: sinusoidal association with symmetric noise.

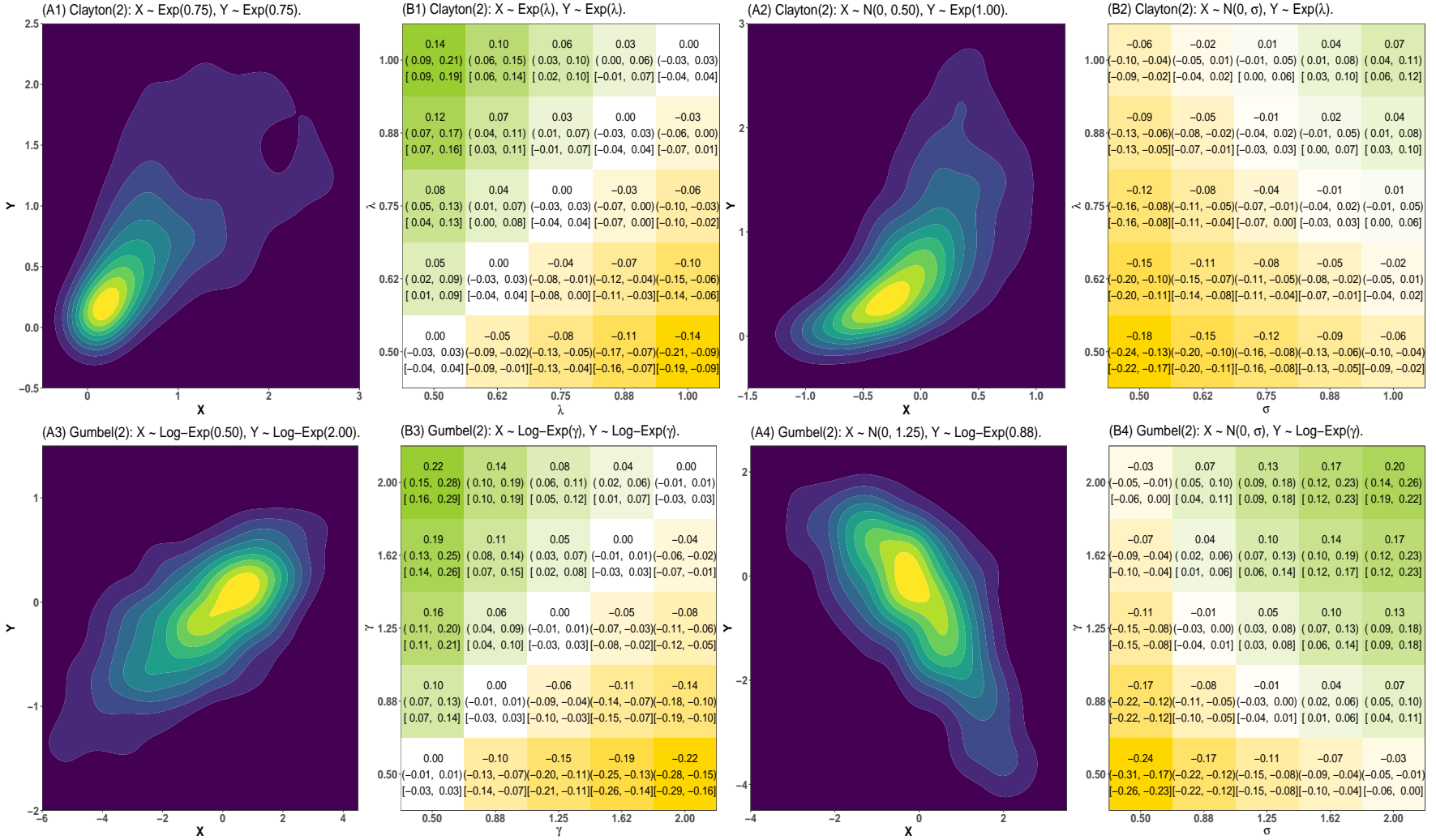


n 250 500 1000

Figure 4.1

Density heatmaps of patterns used to study performance of AMI-based test of asymmetric predictability.

Estimated $\hat{\Delta}$ (estimated 95% C.I.) [theoretical 95% C.I.] reported for specified copula and marginal distributions.



Note:
 (1) Cells are shaded green if X exerts predictive dominance over Y.
 (2) Cells are shaded yellow if Y exerts predictive dominance over X.

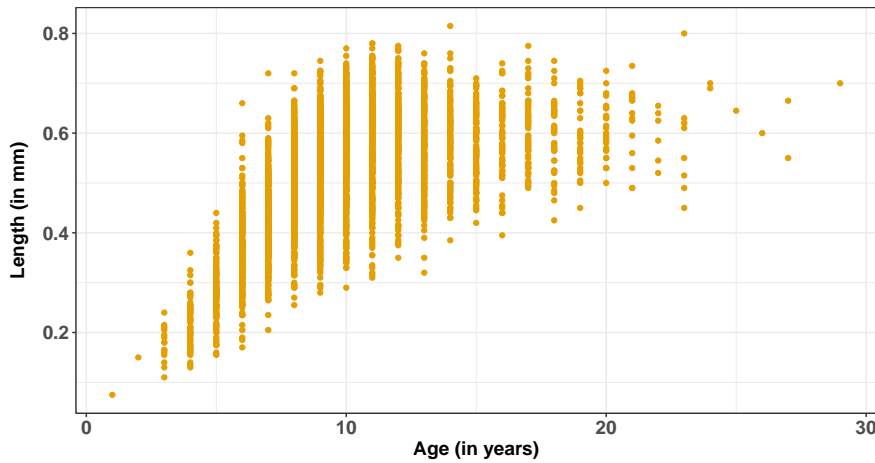
Figure 4.2

Investigating the influence of age on length, diameter, height and weight of Abalone snails (Nash et al., 1994).

Estimated $\hat{\Delta}$ (95% CI) reported for each pair.

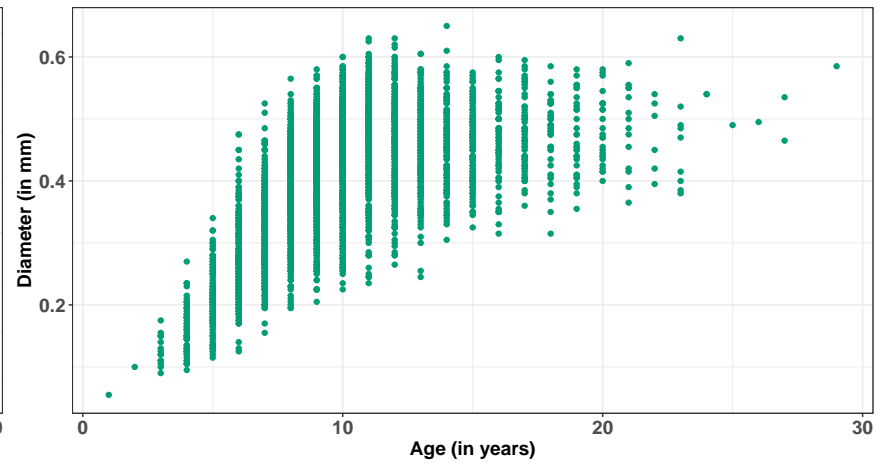
True direction of dependence: Age \rightarrow Length.

Estimated $\hat{\Delta}$ (95% CI): 34.67 (21.08, 48.26), implies age dominates over length.



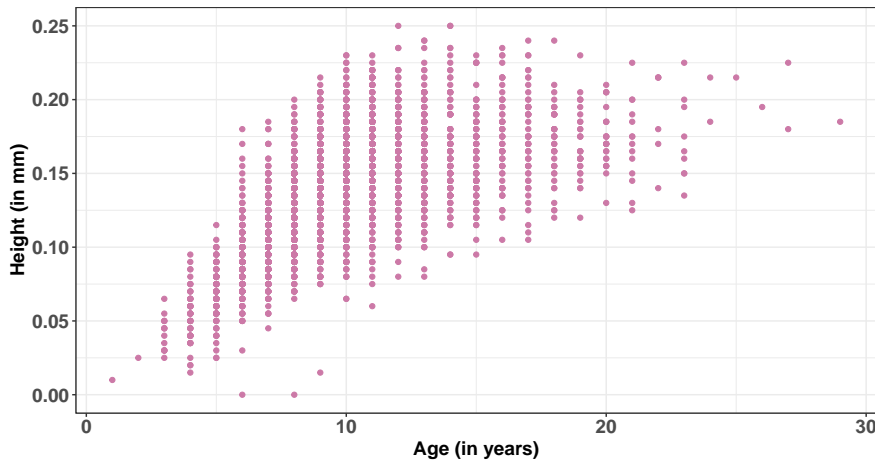
True direction of dependence: Age \rightarrow Diameter.

Estimated $\hat{\Delta}$ (95% CI): 36.97 (23.18, 50.76), implies age dominates over diameter.



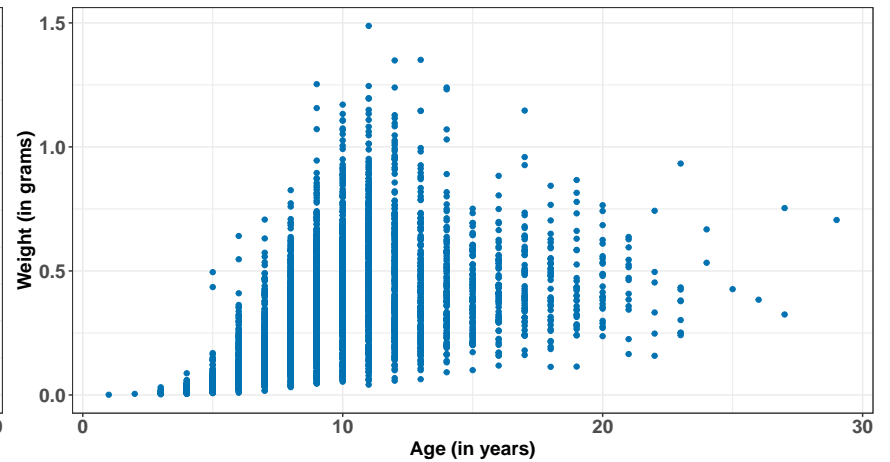
True direction of dependence: Age \rightarrow Height.

Estimated $\hat{\Delta}$ (95% CI): 38.42 (24.6, 52.24), implies age dominates over height.



True direction of dependence: Age \rightarrow Weight.

Estimated $\hat{\Delta}$ (95% CI): 27.67 (19.34, 36.01), implies age dominates over weight.



To improve readability, all figures have been multiplied by a factor of 100.

Figure 5.1

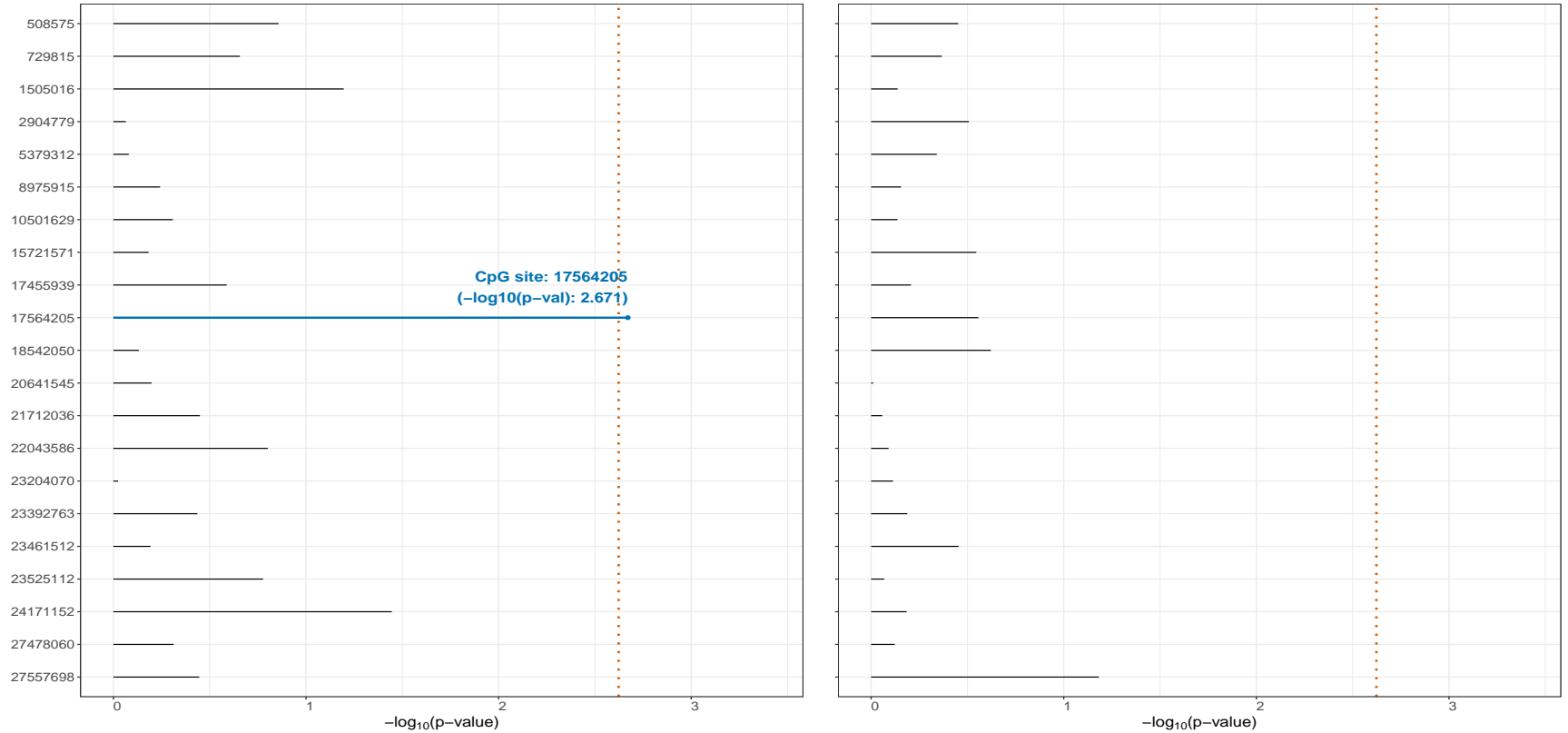
Association and asymmetric predictability between CpG sites of target gene ATP2B1 and blood pressure in ELEMENT cohort study.

Subplots (A1) – (A2) reveal gene-level and CpG site-level association with systolic (SBP) and diastolic blood pressure (DBP) with dotted red line signifying gene-level Bonferroni-adjusted threshold of 5% level of significance.

Subplot (B) reveals asymmetric predictability of CpG sites of target gene ATP2B1 that are significantly (Bonferroni-adjusted) associated with SBP or DBP.

(A1) CCT-based combined p-value for association of ATP2B1 gene with DBP: 0.042

(A2) CCT-based combined p-value for association of ATP2B1 gene with SBP: 0.708



(B) Examining estimated $\hat{\Delta}$ (95% CI) for asymmetric predictability of CpG site 17564205 in ATP2B1 gene that is significantly associated with diastolic BP.

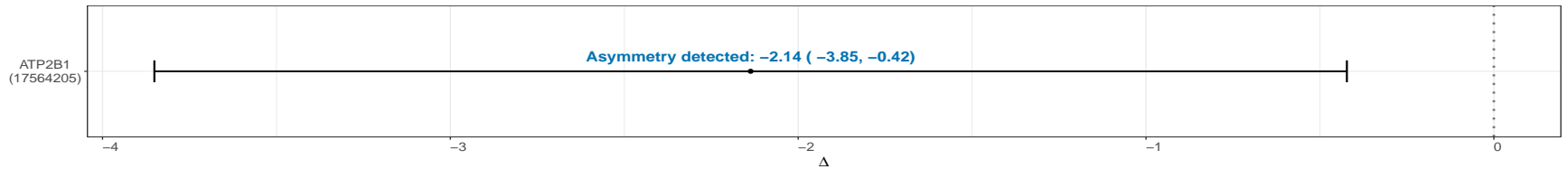


Figure 5.2